M.I.T. Fluid Dynamics Research
Laboratory Report No. 69-1

AN ANALYTIC SOLUTION FOR TWO- AND THREE-DIMENSIONAL WINGS IN GROUND EFFECT

by

Sheila E. Widnall

and

Timothy M. Barrows

MASSACHUSETTS INSTITUTE OF TECHNOLOGY
FLUID DYNAMICS RESEARCH LABORATORY

June 1969

AN ANALYTIC SOLUTION FOR TWO- AND THREE-DIMENSIONAL WINGS IN GROUND EFFECT

Sheila E. Widnall*

and

Timothy M. Barrows**

Massachusetts Institute of Technology

Abstract

The method of matched asymptotic expansions is applied to the problem of a ram wing of finite span in very close proximity to the ground. The general lifting surface problem is shown to be a direct problem, represented by a source-sink distribution on the upper surface of the wing and wake, with concentrated sources around the leading and side edges plus a separate confined channel flow region under the wing and wake. The two-dimensional flat plate airfoil is examined in detail and results for upper and lower surface pressure distribution and lift coefficient are compared with a numerical solution. A simple analytic solution is obtained for a flat wing with a straight trailing edge which has minimum induced drag. To lowest order, this optimally loaded wing is an elliptical wing with a lift distribution which is linear along the chord. The resultant total spanwise lift distribution is parabolic. An expression for the lift coefficient at small clearance and angle of attack, valid for moderate aspect ratio, is derived. The analytic results are compared with numerical results from lifting surface theory for a wing in ground effect; reasonable agreement is obtained.

---

* Assistant Professor, Department of Aeronautics and Astronautics

** Graduate Student, Department of Mechanical Engineering

1. Introduction

The possibility of using aerodynamic forces to support a high speed ground transportation vehicle gives rise to an interesting class of "ram wing" lifting surface problems. A ram wing can be defined as a lifting surface operating in close proximity to a solid boundary. A sketch of various types of ground transportation vehicles which operate in either open or enclosed guideways appears in Figure 1. The finite aspect ratio ram wing, also sketched in Figure 1, can be considered the simplest three-dimensional problem in this class.

Close proximity has definite performance advantages. Very high lift coefficients and lift/drag ratios can be achieve with such vehicles. The optimum lift/drag ratios for a variety of configurations in close proximity were derived (Barrows and Widnall, 1969) by considering the two-dimensional flow in the vortex wake far downstream of the lifting surface. For the ram wing in ground effect, the lowest order solution was shown to be

$$C_{Di} = \frac{C_L^2}{\pi K A R} \tag{1.1}$$

where $K = \frac{2}{3\pi\varepsilon}$, and ε is the clearance at the trailing edge. In ordinary wing theory KAR is called the effective aspect ratio, in this case it goes to infinity as the clearance goes to zero. The spanwise lift distribution for an optimally loaded wing in close proximity to the ground was shown to be parabolic as contrasted with the elliptical distribution for an optimally loaded wing in an infinite fluid.

In the present paper the method of matched asymptotic expansions (cf. Van Dyke, 1964 and Ashley and Landahl, 1965) is used to develop a full three-dimensional lifting surface theory in a series expansion in the clearance parameter ε. The flow in the confined region beneath the wing and trailing vortex wake is joined to the outer flow in the region above the wing through edge flows at the outer boundaries of the wing and wake. The procedure can be extended to cover more complex configurations operating in enclosed or open guideways to obtain analytical predictions of the

aerodynamic characteristics of these vehicles.

2. Problem Formulation - The General Problem

The finite wing in close proximity to the ground in an incompressible flow is sketched in Figure 2. There are two possible versions of this problem for the region beneath the wing, the linear and nonlinear problem. In the linear problem, the displacements of the under surface must be small in comparison to the clearance to chord ratio. This version is compatible with linearized lifting surface theory in which the lowest order solution everywhere is a free stream and the upwash boundary conditions are satisfied on the mean plane of the wing, at a height ε above the ground. In the nonlinear problem, the displacements of the under surface are of the order of the clearance. The lowest order solution for the flow beneath the wing is not a uniform stream and the flow tangency boundary condition must be satisfied on the actual lower surface. This latter problem is more difficult and is currently under investigation. The linear problem will be examined in this paper and the results compared with numerical lifting surface theory.

The wing upper and lower surfaces are described by

$$\begin{aligned} S_\ell(x,y,z) &= z - \varepsilon \bar{f}_\ell(x,y) = 0 \qquad \text{on lower surface} \\ S_u(x,y,z) &= z - \varepsilon \bar{f}_u(x,y) = 0 \qquad \text{on upper surface} \end{aligned} \tag{2.1}$$

where $\bar{f}_{u,\ell}(x,y) = 1 + \frac{\alpha}{\varepsilon}\bar{g}_{u,\ell}(x,y)$. $\bar{g}_{u,\ell}(x,y)$ is an $0(1)$ function describing the distribution of camber, angle of attack and thickness on the airfoil.

The boundary condition of flow tangency is

$$\nabla\Phi\cdot\nabla S_{u,\ell}(x,y,z) = 0 \text{ on } S_{u,\ell}(x,y,z) = 0 \tag{2.2}$$

On the ground we require

$$\frac{\partial\Phi}{\partial z} = 0 \tag{2.3}$$

where Φ is the velocity potential, satisfying Laplace's equation

$$\nabla^2\Phi = 0 \tag{2.4}$$

To determine a perturbation solution valid for the region beneath the wing, the z coordinate is stretched. The notation Φ^c for "channel flow" will be used for this

region. Let

$$\bar{z} = z/\varepsilon \text{ and } \frac{\partial \phi^c}{\partial \bar{z}} = \varepsilon \frac{\partial \phi}{\partial z} \tag{2.5}$$

The boundary condition of flow tangency on the lower surface for ϕ^c is

$$\frac{\partial \phi^c}{\partial \bar{z}} = \varepsilon\alpha \nabla_{2D} \bar{g}_\ell(x,y)\cdot\nabla_{2D}\phi^c \text{ at } \bar{z} = 1 + \frac{\alpha}{\varepsilon}\bar{g}_\ell(x,y) \tag{2.6}$$

where ∇_{2D} is the two-dimensional operator $\bar{i}\frac{\partial}{\partial x} + \bar{j}\frac{\partial}{\partial y}$.

There are two small parameters in this problem α, the angle of attack, and ε, the clearance. If $\alpha \sim O(\varepsilon)$, the boundary conditions must be satisfied on the actual under surface of the wing, if $\alpha \sim o(\varepsilon)$, a Taylor series expansion of the boundary conditions about $\bar{z} = 1$ is permitted (Van Dyke, 1964) and an ordinary linear lifting surface problem is obtained. To compare with numerical lifting surface theory, only terms linear in α would be appropriate.

An asymptotic expansion of the form

$$\begin{aligned}\phi^c(x,y,\bar{z}) = {\phi_o}^c + \frac{\alpha}{\varepsilon}{\phi_1}^c + \alpha f_1(\varepsilon){\phi_2}^c + \alpha{\phi_3}^c + \ldots \\ + \alpha\varepsilon{\phi_4}^c + \alpha\varepsilon^2 f_1(\varepsilon){\phi_5}^c + \alpha\varepsilon^2{\phi_6}^c \ldots\end{aligned} \tag{2.7}$$

or

$$\phi^c(x,y,\bar{z}) = x + \alpha\phi^c$$

will be assumed. In the linearized problem ${\phi_o}^c$ beneath the wing is simply x, the uniform free stream. In the actual development of the solution, the next functions of ε would be determined at each stage in the process. From matching with the edge solutions, $f_1(\varepsilon)$ turns out to be $\ell n(1/\varepsilon)$. ${\phi_1}^c$, ${\phi_2}^c$ and ${\phi_3}^c$ will determine the lift coefficient on the wing to $O(\alpha)$. To determine the equations which ${\phi_1}^c$, ${\phi_2}^c$ and ${\phi_3}^c$ satisfy we must determine the form of ${\phi_4}^c$, ${\phi_5}^c$ and ${\phi_6}^c$, respectively.

Before examining further the flow beneath the wing we consider the outer flow, the flow above the wing in the limit $\varepsilon = 0$, sketched in Figure 3.

The outer flow is a straightforward thin wing flow in both the linear and nonlinear problems

$$\phi^\circ = x + \alpha\phi_1^\circ + \ldots \tag{2.8}$$

Interestingly enough, however, the outer flow is not a lifting problem but a rather intriguing thickness problem, i.e. the outer flow is a direct rather than an indirect problem. Figure 4 indicates the boundary conditions to be satisfied on the ground plane, $z = 0$.

$$\frac{\partial\phi_1^\circ}{\partial z} = -\frac{\partial\bar{g}_u}{\partial x} \qquad \text{at } z = 0 \text{ on } S,$$

$$\frac{\partial\phi_1^\circ}{\partial z} = -\alpha_i(x,y) \text{ at } z = 0 \text{ on } W, \tag{2.9}$$

and for $z = 0$ off of W and S

$$\frac{\partial\phi_1^\circ}{\partial z} = 0$$

where S and W are the projections of the wing and wake surfaces on $z = 0$. $\alpha_i(x,y)$ is the induced downwash in the wake due to the trailing vortex system. The singularities used to satisfy these boundary conditions are sources and sinks rather than the elementary horseshoe vortices which appear for the lifting problem for a wing far from the ground. In addition to the distribution of sources and sinks there are eigensolutions, concentrated sources (or sinks) of unknown strength located around the leading edge of the wing and side edges of the wake. These are absent at the trailing edge of the wing to lowest order because of the Kutta condition. Their purpose is to replace the fluid which has been removed by the excess of distributed sinks on the wing and wake surfaces. All of the properties of the outer flow potential ϕ_1° can be found by solving lower order inner problems. The important feature of the outer flow is its very weak, $O(\alpha)$, influence on the inner flow. For the linearized problem this means that the zeroth order flow beneath the wing is a uniform stream and that $\phi_1^c = 0$ at the leading edge and $\frac{\partial\phi_1^c}{\partial x} = 0$ at

the trailing edge.

We now state the sequence of problems and boundary conditions associated with the flow beneath the wing and wake.

With the stretching of the z coordinate as indicated in (2.5) the governing equation becomes

$$\frac{1}{\varepsilon^2}\frac{\partial^2\phi^c}{\partial\bar{z}^2} + \nabla_{2D}^2\phi^c = 0 \tag{2.10}$$

Applying this equation to the assumed form of ϕ^c of (2.7) and equating like functions of ε gives a very simple set of partial differential equations for the ϕ_n^c's.

$$\frac{\partial^2\phi_n^c}{\partial\bar{z}^2} = 0 \qquad 0 \le n \le 3 \tag{2.11}$$

Since $\frac{\partial\phi^c}{\partial\bar{z}} = 0$ at $\bar{z} = 0$, the solutions to these equations are simply functions of x and y.

$$\phi_n^c = \phi_n^c(x,y) \qquad 0 \le n \le 3 \tag{2.12}$$

For the next order solutions the governing equations are

$$\begin{aligned}
\frac{\partial^2\phi_4^c}{\partial\bar{z}^2} &= -\nabla_{2D}^2\,\phi_1^c(x,y)\\
\frac{\partial^2\phi_5^c}{\partial\bar{z}^2} &= -\nabla_{2D}^2\,\phi_2^c(x,y)\\
\frac{\partial^2\phi_6^c}{\partial\bar{z}^2} &= -\nabla_{2D}^2\,\phi_3^c(x,y)
\end{aligned} \tag{2.13}$$

Since $\frac{\partial\phi^c}{\partial\bar{z}}$ at $\bar{z} = 0$, the solutions for ϕ_4^c, ϕ_5^c, and ϕ_6^c are

$$\begin{aligned}
\phi_4^c &= -\frac{\bar{z}^2}{2}\nabla_{2D}^2\,\phi_1^c(x,y) + \tilde{\phi}_4^c(x,y)\\
\phi_5^c &= -\frac{\bar{z}^2}{2}\nabla_{2D}^2\,\phi_2^c(x,y) + \tilde{\phi}_5^c(x,y)\\
\phi_6^c &= -\frac{\bar{z}^2}{2}\nabla_{2D}^2\,\phi_3^c(x,y) + \tilde{\phi}_6^c(x,y)
\end{aligned} \tag{2.14}$$

where $\tilde{\phi}_n^c$ is, at this stage, some arbitrary function of x and y. We now apply the flow tangency conditions on the undersurface of the wing. This will give a set of

equations for the unknown functions ϕ_n^c, n = 1, 2, 3. The boundary conditions for these equations are obtained by matching with the outer flow around the edges of the wing and wake surfaces through an edge flow region. The flow tangency condition of (2.6) expanded as a Taylor series about $\bar{z} = 1$ becomes

$$\frac{\partial \phi^c}{\partial \bar{z}}(x,y,1) + \frac{\partial^2 \phi^c}{\partial \bar{z}^2}(x,y,1)\,\frac{\alpha}{\varepsilon}\,\bar{g}_\ell(x,y) + \ldots = \varepsilon\alpha\,\nabla_{2D}\,\bar{g}_\ell(x,y)\cdot\nabla_{2D}\,\phi^c(x,y,1) + \ldots \tag{2.15}$$

Using the assumed form for Φ^c and equating like functions of α and ε, the boundary conditions for ϕ_4^c become

$$\frac{\partial \phi_4^c}{\partial \bar{z}} = \frac{\partial \bar{g}_\ell}{\partial x} \qquad \text{at } \bar{z} = 1 \tag{2.16}$$

The boundary conditions for ϕ_5^c and ϕ_6^c are

$$\frac{\partial \phi_5^c}{\partial \bar{z}} = 0, \qquad \frac{\partial \phi_6^c}{\partial \bar{z}} = 0 \text{ at } \bar{z} = 1 \tag{2.17}$$

Using the solutions for ϕ_4^c, ϕ_5^c, and ϕ_6^c of (2.14) in (2.16) we obtain essentially a set of partial differential equations for ϕ_1^c, ϕ_2^c, and ϕ_3^c. For $\phi_1^c(x,y)$

$$\nabla_{2D}^2\,\phi_1^c(x,y) = -\frac{\partial \bar{g}_\ell}{\partial x}(x,y) \tag{2.19}$$

Physically this equation can be interpreted as conservation of mass in the two-dimensional region beneath the wing with known distributed mass addition provided by the flow tangency boundary condition on the lower surface.

From the boundary conditions of (2.17) and the relation between ϕ_2^c and ϕ_5^c and ϕ_6^c and ϕ_3^c given by (2.14), ϕ_2^c and ϕ_3^c satisfy Laplace's equation

$$\nabla_{2D}^2\,\phi_2^c(x,y) = 0, \qquad \nabla_{2D}^2\,\phi_3^c(x,y) = 0 \tag{2.20}$$

i.e. two-dimensional potential flow under the wing.

Across the trailing vortex wake, the discontinuity in potential, $\Delta\phi$, must be a function of y only. Since the outer flow perturbations are $O(\alpha)$, the perturbation

potentials ϕ_1^c and ϕ_2^c, which are valid beneath the wake for distances behind the trailing edge greater than ε, are likewise functions of y only. However, ϕ_3^c is in general a function of x and y since the outer flow potential ϕ_1° which contributes to $\Delta\phi(y)$ is a function of x near the wing. In the wake, (2.19) and (2.20) become

$$\begin{aligned} \frac{d^2\phi_1^c}{dy^2} &= \alpha_i(y) \\ \frac{d^2\phi_2^c}{dy^2} &= \alpha_{2i}(y) \\ \nabla^2\phi_3^c &= \alpha_{3i}(x,y) \end{aligned} \tag{2.21}$$

These equations are interpreted as equations for the induced downwash α_i for a known vortex strength in the wake; α_{2i} and α_{3i} are higher order contributions .

To summarize, the relations, equations, and flow tangency boundary conditions have yielded a set of partial differential equations for the lowest order solutions ϕ_1^c to ϕ_3^c. The equation governing ϕ_1^c is that of conservation of mass in the two-dimensional channel beneath the wing with a known mass addition. The equation governing the other functions is simply Laplace's equation for two-dimensional potential flow under the wing with no mass addition. From these solutions we can find the expression for the pressure on the underside of the wing. We can also solve for the structure of the wake and the strength of the edge sources in the outer flow. Inspection of the outer flow and edge flow solutions indicates that the boundary condition to be satisfied on the edges of the two-dimensional channel which represents the underside of the wing and wake are

$$\begin{aligned} \phi_1^c &= 0 \qquad \text{at the leading and side edges,} \\ \frac{\partial\phi_1^c}{\partial x} &= 0 \qquad \text{at the trailing edge.} \end{aligned} \tag{2.22}$$

The boundary conditions on ϕ_2^c and ϕ_3^c on the edges bounding the confined region under the wing are more complex and must be obtained from matching with the outer flow potential ϕ° through the edge flow solutions.

3. Edge Flow Solutions

Matching of the flows underneath and above the wing requires solutions which are valid near the leading, trailing, and side edges. For a two-dimensional flow in the xz plane, these are obtained using the magnified complex variable

$$Y = \bar{x} + i\bar{z}$$

where $\bar{x} = x/\varepsilon$, and $\bar{z} = z/\varepsilon$.

That is, we now magnify x as well as z in order to focus on the properties of the region near the edge. This will be called the inner region in the usual sense of asymptotic expansions. For a general three-dimensional wing, $\bar{x}$ would be replaced by a local coordinate $\bar{n}$ normal to the edge.

The edge flows may be written in the following form (see Figure 5)

$$\phi^i = \varepsilon\, \phi_A + a_1\, \phi_B + a_2\, \bar{x} + a_3 \tag{3.1}$$

where ϕ^i = potential in the inner region

ϕ_A = solution which satisfies the downwash condition $\partial\phi/\partial\bar{z} = -1$ on the wing

ϕ_B = eigensolution with homogeneous boundary conditions -- no velocity normal to the wing or the ground

$\bar{x}$ = a local free stream

a_n = constants to be determined by matching

The solutions ϕ_A and ϕ_B may both be obtained using the following transformation

$$Y = \eta + \frac{1}{\pi}\left[1 + e^{\eta\pi}\right] \tag{3.2}$$

where $\eta = \xi + i\zeta$

This transformation leaves the ground unchanged and transforms the wing and its image onto the lines $\zeta = \pm 1$. To obtain the eigensolution, transform the complex potential for a uniform flow in the η plane onto the Y plane

$$F(\eta) = \phi_B + i\psi_B = U\eta \tag{3.3}$$

where U = constant.

Eliminating η between (3.2) and (3.3) gives

$$Y = \frac{F}{U} + \frac{1}{\pi}\left[1 + e^{(F/U)\pi}\right] \tag{3.4}$$

Since $\psi_B = U$ on $\bar{z} = 1$, we can substitute $Y = \bar{x} + i$ and $F = \phi_B + iU$ and obtain for the wing

$$\bar{x} = \frac{\phi_B}{U} + \frac{1}{\pi}\left[1 - e^{\pi\phi_B/U}\right] \tag{3.5}$$

This gives an inverse relation between $\bar{x}$ and ϕ_B on the wing.

For matching it is only necessary to invert this relation for the asymptotic cases of large $\bar{x}$. As $\phi_B \to \infty$ the exponential dominates and we obtain

$$\begin{aligned} \bar{x} &\sim -\frac{1}{\pi} \exp \pi\, \phi_B/U \\ \phi_{Bu} &\sim \frac{U}{\pi} \ell n|\pi\bar{x}| \end{aligned} \tag{3.6}$$

Here the subscript u has been added since this represents the potential on the upper surface of the wing. For the lower surface $\phi \to -\infty$. The exponential decays giving

$$\phi_{B\ell} \sim U(\bar{x} - \frac{1}{\pi}) \tag{3.7}$$

These asymptotic limits must match the outer flow and the flow under the wing respectively.

The solution for ϕ_A follows a similar development except that the complex velocity is transformed, rather than the complex potential. The required boundary conditions are obtained from simple corner flow in the η plane. Take

$$W(\eta) = u - iv = \eta$$

This is transformed to the Y plane using (3.2)

$$Y = W + \frac{1}{\pi}\left[1 + e^{\pi W}\right] \tag{3.8}$$

On the wing, $v = -1$, so that $W = u + i$ and $Y = \bar{x} + i$. Substituting

$$\bar{x} = u + \frac{1}{\pi}\left[1 - e^{\pi u}\right] \tag{3.9}$$

As before, we obtain asymptotic limits and attach appropriate subscripts:

$$u_u \sim \frac{1}{\pi}\ \ell n|\pi\bar{x}| \tag{3.10}$$

$$u_\ell \sim \bar{x} - \frac{1}{\pi} \tag{3.11}$$

The corresponding asymptotic values of the potential are as follows:

$$\phi_{Au} \sim \frac{\bar{x}}{\pi} \ell n(\pi\bar{x}) - \frac{\bar{x}}{\pi} \tag{3.12}$$

$$\phi_{A\ell} \sim \frac{\bar{x}^2}{2} - \frac{\bar{x}}{\pi} \tag{3.13}$$

4. The Two-Dimensional Wing in Ground Effect

The use of the edge solutions is best illustrated by the problem of a flat plate airfoil of infinite span in close proximity to the ground. The perturbation potential ϕ_1°, introduced in (2.8) must have unit downwash on the wing and, in addition, must satisfy global mass conservation. The downwash condition is satisfied by a lineal distribution of sinks; to satisfy mass conservation one can add eigensolutions, concentrated sources at the leading and trailing edges with a total mass flow equal to the mass intake of the sinks. However the Kutta condition serves to rule out the possibility of singularities at the trailing edge, so that the leading edge must have a single source of strength two. The complex potential for this flow can be written directly as

$$F(Y) = -\frac{1}{\pi} \int_0^1 \ell n(Y - Y_1)\, dY_1 + \frac{1}{\pi} \ell nY \tag{4.1}$$

The perturbation potential evaluated on the upper surface of the wing, $z = 0$, is then

$$\phi_1^\circ = \frac{1}{\pi} \left[(x - 1)\, \ell n\left(\frac{1-x}{x}\right) + 1\right] \tag{4.2}$$

For the flow underneath the wing (2.19) and (2.20) become

$$\frac{d^2\phi_1{}^c}{dx^2} = 1$$

$$\frac{d^2\phi_2{}^c}{dx^2} = \frac{d^2\phi_3{}^c}{dx^2} = 0 \tag{4.3}$$

The complete solution for the perturbation potential ϕ^c, where

$$\phi^c = \frac{1}{\epsilon}\, \phi_1{}^c + f_1(\epsilon)\, \phi_2{}^c + \phi_3{}^c \tag{4.4}$$

can then be written

$$\phi^c = \frac{x^2}{2\epsilon} + G(\epsilon)x + H(\epsilon) \tag{4.5}$$

with the unknown functions $G(\epsilon)$ and $H(\epsilon)$ to be determined by matching.

At this stage one can formulate a strategy for matching the various regions of the flow. This will be done in the following four steps as shown in Figure 6:

1. Apply the Kutta condition at the trailing edge and match the edge solution to the outer flow.

2. Match the channel flow to the trailing edge region. The velocity here must match to the velocity above the trailing edge, which gives a boundary condition for $d\phi^c/dx$ at the trailing edge. There is an unknown discontinuity in the potential, however, due to the circulation.

3. Match the outer flow to the edge flow above the leading edge.

4. Match the edge flow to the channel flow below the leading edge. This gives the boundary condition for ϕ^c at the leading edge.

Step 1. The Kutta condition at the trailing edge is imposed by stating that no eigensolution exists, since this solution gives infinite velocity at the edge. The solution is $\varepsilon\phi_A$, satisfying the downwash boundary condition, plus a uniform stream and a constant. The trailing edge variable $\bar{x}_T$ is used as in Figure 6.

$$\phi_T{}^i = \frac{1}{\pi}[c_1(\varepsilon)\ \varepsilon\bar{x}_T + c_2(\varepsilon)] + \varepsilon\phi_A \tag{4.5}$$

where the factors $1/\pi$ and ε are written for convenience.

This is written in outer variables and expanded to 0(1) for the upper surface of the wing using (3.12)

$$\phi_{Tu}^{io} = \frac{1}{\pi}\left[x_T(\ell n\, x_T + \ell n\, \frac{\pi}{\varepsilon} + c_1 - 1) + c_2\right] \tag{4.6}$$

ϕ_{Tu}^{io} is the outer limit of the inner solution near the trailing edge on the upper surface of the wing. The outer solution in the inner variable $\bar{x}_T$ is obtained from (4.2) with $x = 1 + \varepsilon\bar{x}_T$

$$\phi_T{}^o = \frac{1}{\pi}\left[\varepsilon\bar{x}_T \ell n\left|\frac{\varepsilon\bar{x}_T}{1 + \bar{x}_T}\right| + 1\right] \tag{4.7}$$

Expanded to $0(\varepsilon)$ and re-expressed in outer variables, this is

$$\phi_T^{oi} = \frac{1}{\pi}\left[x_T\ \ell n|x_T| + 1\right] \tag{4.8}$$

Using the limit matching principle, ϕ^{oi} must equal ϕ^{io} which gives

$$c_1 = 1 - \ell n(\pi/\varepsilon)$$
$$c_2 = 1 \tag{4.9}$$

Step 2. Beneath the trailing edge the potential is also given by (4.5) with the addition of the potential jump across the wake due to the circulation Γ.

$$\phi^i_{T\ell} = \frac{1}{\pi}\left[(1 - \ell n\tfrac{\pi}{\varepsilon})\varepsilon\bar{x}_T + 1\right] - \Gamma + \varepsilon\phi_A \tag{4.10}$$

This is expressed in the channel (or outer) variable x and expanded to 0(1) for the region below the wing using (3.13). The resulting expression $\phi^{ic}_{T\ell}$ is interpreted as the limit of the inner trailing edge solution as it tends toward channel flow.

$$\phi^{ic}_{T\ell} = \frac{x_T^2}{2\varepsilon} + \frac{1}{\pi}\left[-x_T \ell n\tfrac{\pi}{\varepsilon} + 1\right] - \Gamma \tag{4.11}$$

This limit must equal the channel flow limit at the trailing edge. Since the value of the channel flow velocity rather than the potential is fixed by the Kutta condition, (4.11) gives the boundary condition at x = 1,

$$\frac{d\phi}{dx}^c = -\frac{1}{\pi}\,\ell n\,\frac{\pi}{\varepsilon}$$

Also

$$f_1(\varepsilon) = \ell n(1/\varepsilon) \tag{4.12}$$

The boundary conditions for the individual terms become

$$\frac{d\phi_1}{dx}^c = 0$$
$$\frac{d\phi_2}{dx}^c = -\frac{1}{\pi} \tag{4.13}$$
$$\frac{d\phi_3}{dx}^c = -\frac{1}{\pi}\,\ell n\pi$$

Step 3. The matching over the leading edge is similar to step 1, except that the eigensolution is now allowed and all solutions are written in the leading edge variables. The solutions for the edge region are obtained from (3.5) and (3.9) (with appropriate sign changes, since the picture in Figure 5 must be reversed).

The potential in the inner leading edge region is, using (3.1)

$$\phi^i = \phi_B + \frac{1}{\pi}\left[c_3(\varepsilon)\varepsilon\bar{x} + c_4(\varepsilon)\right] + \varepsilon\phi_A \tag{4.14}$$

The matching to the outer solution in the region above the leading edge proceeds by expressing ϕ^i in the outer variable x and expanding to 0(1) above the edge.

$$\phi^{io} \sim \frac{1}{\pi}[U(\varepsilon)\ell n\frac{\pi x}{\varepsilon} + c_3 x + c_4 - (x\ell n\frac{\pi x}{\varepsilon} - x)] \tag{4.15}$$

It is useful to write $U(\varepsilon) = U_o + \varepsilon U_1$. When this is done and the resulting expression rearranged we obtain to O(1)

$$\phi^{io} \sim \frac{1}{\pi}[U_o \ell nx - x\ell nx + x(1 - \ell n\frac{\pi}{\varepsilon} + c_3) + U_o \ell n\frac{\pi}{\varepsilon} + c_4] \tag{4.16}$$

The inner limit of the outer solution can be obtained from (4.2).

$$\phi^{oi} = \frac{1}{\pi}[\ell nx - x\ell nx + x + 1] \tag{4.17}$$

Comparison between (4.16) and (4.17) gives

$$U_o = 1$$

$$c_3 = \ell n\pi/\varepsilon$$

$$c_4 = 1 - \ell n\pi/\varepsilon$$

Step 4. For the final step in the matching, the inner flow near the leading edge is expanded into the region under the wing giving a second boundary condition to determine ϕ^c and hence Γ.

The expression for ϕ^i given by (4.14) is now expanded in outer or channel variables below the wing using the asymptotic forms for ϕ_A and ϕ_B valid beneath the wing given by (3.7) and (3.13). To O(1)

$$\phi^{ic} = \frac{x^2}{2\varepsilon} - \frac{x}{\varepsilon} - xU_1 + \frac{x}{\pi}(1 + \ell n\frac{\pi}{\varepsilon}) - \frac{1}{\pi}\ell n\frac{\pi}{\varepsilon} \tag{4.18}$$

Applying the limit matching principle to (4.18) gives a boundary condition for ϕ^c at the leading edge

$$\phi^c(0) = -\frac{1}{\pi}\ell n\frac{\pi}{\varepsilon} \tag{4.19}$$

As in (4.13), the boundary conditions for the individual terms are

$$\begin{aligned} \phi_1{}^c(0) &= 0 \\ \phi_2{}^c(0) &= -\frac{1}{\pi} \\ \phi_3{}^c(0) &= -\frac{1}{\pi}\ell n\pi \end{aligned} \tag{4.20}$$

The boundary condition of (4.12) and (4.19) determines the final expression for ϕ^c,

$$\phi^c = \frac{x^2}{2\varepsilon} - \frac{x}{\varepsilon} - \frac{x}{\pi}\ell n\frac{\pi}{\varepsilon} - \frac{1}{\pi}\ell n\frac{\pi}{\varepsilon} \tag{4.21}$$

By comparing (4.21), (4.11) and (4.18) we obtain

$$U_1 = \frac{1}{\pi}[2\ \ell n\frac{\pi}{\varepsilon} + 1]$$

and $$\Gamma = \frac{1}{2\varepsilon} + \frac{1}{\pi}[2\ \ell n\frac{\pi}{\varepsilon} + 1] \tag{4.22}$$

Remembering that Γ as written here is the circulation normalized by α, the lift coefficient is

$$C_L = 2\Gamma\alpha = \frac{\alpha}{\varepsilon} + \frac{2\alpha}{\pi}\ (2\ell n\frac{\pi}{\varepsilon} + 1) \tag{4.23}$$

A uniformly valid composite solution for the flow above the wing can be constructed as follows:

$$\phi = (\phi^i_{Tu} - \phi^{io}_T) + (\phi^i - \phi^{io}) + \phi^o$$

A similar formula holds below the wing with ϕ^c substituted for ϕ^o and $\phi^i_{T\ell}$ substituted for ϕ^i_{Tu}, etc.

The upper and lower surface pressure distributions predicted from these composite solutions were compared with a numerical linearized thin airfoil solution which used a Glauert series with six terms and nineteen downwash control points. Boundary conditions were satisfied in the least squares sense and the ground was represented using the method of images. Figure 7 shows the comparison for a height to chord ratio $\varepsilon = .1$; the agreement is essentially perfect. The pressure under the wing is linear over most of the chord with the edge flow solutions providing the proper local behavior at the leading and trailing edges. The first order solution is also indicated in Figure 7 for later comparison with the three dimensional results. Figure 8 shows the comparison for $\varepsilon = .3$, Figure 9 for $\varepsilon = .5$. The agreement is remarkably good for this latter clearance, considering that the "inner edge" regions for this case are so large that they essentially overlap.

The lift coefficient to 0(1) given by (4.23) is shown in Figure 10 in comparison with the numerical results. It is necessary to plot $C_L\varepsilon/\alpha$ versus ε in order to clearly indicate the behavior at $\varepsilon = 0$. Strangely enough, Figure 10 does not reflect the same accuracy as the pressure coefficient results. This is suprising as, presumably, (4.23) simply represents an analytic integration of pressure distribution. The resolution of this anomaly is obtained by proceeding to the next higher order, i.e., $0(\varepsilon\ \ell n\ \varepsilon)$. It is found that a source and a doublet must be

added to the leading edge in the outer flow, and a sink to the trailing edge:

$$\phi^o = \frac{1}{\pi}\left[(x - 1)\ \ell n\left(\frac{1-x}{x}\right) + 1\right] + \frac{\varepsilon}{\pi^2}\ \ell n\frac{\pi}{\varepsilon}\left[\ell nx - \ell n(1 - x) + \frac{1}{x}\right] \tag{4.24}$$

It is not worthwhile to go into the details of the matching which follow the previous analysis fairly closely. A small increment to the circulation is obtained.

$$\Gamma = \frac{1}{2\varepsilon} + \frac{1}{\pi}\ (2\ell n\frac{\pi}{\varepsilon} + 1) + \frac{\varepsilon}{\pi^2}(4\ell n\frac{\pi}{\varepsilon} + 2\ell n^2\ \frac{\pi}{\varepsilon}) \tag{4.25}$$

The important point is that nearly all of the difference between (4.23) and (4.25) arises from constants which are added to ϕ^c as the solution is carried out to $O(\varepsilon\ell n\varepsilon)$ and $O(\varepsilon\ell n^2\varepsilon)$. The velocity and pressure under the wing are unaffected to this next order. These constants represent additional contributions to the total lift from the leading edge region. The addition of these higher order constants to ϕ^c considerably improves the agreement with the numerical solution, as shown in Figure 10.

The above analysis provides a base for the examination of the three-dimensional lifting surface problem. It has revealed the nature of the flow beneath the wing, the nature of the edge flow regions, and the influence of the outer flow. Comparison with the numerical solution indicates the accuracy of the predicted pressure distribution and total lift.

5. Three-Dimensional Flat Wing Ground Effect

We now consider the case of a flat plate wing with a straight trailing edge close to the ground.

To lowest order, the expressions for the velocity potential above and below the wing are

$$\phi^\circ = x + \alpha\phi_1{}^\circ + \ldots$$

and (5.1)

$$\phi^c = x + \frac{\alpha}{\varepsilon}\phi_1{}^c + \ldots$$

$\phi_1{}^c$ which determines the essential features of the flow is unaffected by the outer flow. For a flat wing, the function describing the shape of the lower surface is

$$\bar{g}_{\ell}(x,y) = -x \tag{5.2}$$

Equation (2.19) becomes

$$\nabla^2_{2D}\, \phi_1^{\,c}(x,y) = 1 \tag{5.3}$$

for the flow under the wing, with boundary conditions given by (2.22). This problem is sketched in Figure 11. The flow tangency condition adds a net mass flow to the region under the wing. Because of the Kutta condition this flow cannot escape at the trailing edge but must go forward and escape out the leading and side edges. Thus the velocity under the wing is lower than free stream and lift is produced.

The solution to (5.3) is

$$\phi_1^{\,c} = \frac{x^2 + y^2}{4} + \phi_{2D}(x,y) + C \tag{5.4}$$

where ϕ_{2D} is any two-dimensional potential flow function and C is a constant. The form of the particular solution and the trailing edge boundary condition suggest the function $\phi_{2D} = A\,[x^2 - y^2]$, the potential function for corner flow. This form of $\phi_1^{\,c}$ gives a parabolic spanwise lift distribution which for a wing in ground effect gives minimum induced drag.

If we take an inverse approach choosing $\phi_1^{\,c}$ and solving for the wing planform which has minimum induced drag, the potential for the optimally loaded wing becomes

$$\phi_1^{\,c} = \frac{x^2 + y^2}{4} + A\,[x^2 - y^2] + C \tag{5.5}$$

$A = 1/4$ corresponds to an infinite aspect ratio wing in ground effect, $A = -1/4$ corresponds to a wing of zero aspect ratio, although the theory is not valid for $AR \sim O(\varepsilon)$. The equation for $\phi_1^{\,c}$ can be manipulated into the form

$$\phi_1^{\,c} = [A + \tfrac{1}{4}] \left[x^2 + \frac{y^2[\frac{1}{4} - A]}{[\frac{1}{4} + A]} - 1 \right] \tag{5.6}$$

where C has been chosen to satisfy the leading edge boundary condition at $x = -1$, $y = 0$.

Applying the boundary condition $\phi_1^c = 0$ to the entire leading edge gives the equation for the leading edge

$$x_{LE}^2 + \left(\frac{y_{LE}}{b}\right)^2 = 1 \tag{5.7}$$

which is the equation of an ellipse with $b = \left(\frac{\frac{1}{4} + A}{\frac{1}{4} - A}\right)^{\frac{1}{2}}$.

After solving for A, the potential ϕ_1^c for a flat elliptical wing becomes

$$\phi_1^c = \frac{b^2}{2(b^2+1)} \left[x^2 + (y/b)^2 - 1\right] \tag{5.8}$$

where b is the semi-span/chord ratio. In the wake $\phi_1^c(y)$ has the value

$$\phi_1^c = \frac{b^2}{2(b^2+1)} \left[(y/b)^2 - 1\right] \tag{5.9}$$

The spanwise distribution of circulation to this order is $\Gamma(y) = -\frac{\alpha}{\varepsilon} \phi_1^c(y)$

$$\Gamma(y) = \left(\frac{\alpha}{\varepsilon}\right) \frac{1}{2} \frac{b^2}{(b^2+1)} \left(1 - (y/b)^2\right) \tag{5.10}$$

since the outer flow perturbation are $0(\alpha)$.

The induced downwash $\alpha_i(y)$ as given by (2.21) is constant in the wake and of magnitude

$$\alpha_i = \frac{1}{b^2+1} \tag{5.11}$$

For b approaching infinity, α_i goes to zero which is the proper limit for infinite aspect ratio; for b approaching zero, α_i goes to one, the slender-body limit.

Figure 11 shows the flow perturbation associated with this solution for flat elliptical wing.

To this order of magnitude, all lift comes from the increased pressures on the bottom of the wing. Figure 12 shows a sketch of the lift distribution. As in the two-dimensional case, the distribution of lift is linear along the chord to lowest order, although at a reduced magnitude due to the finite span. The spanwise lift distribution produced by the elliptical wing is parabolic because a lift distribution which is linear with the same slope along every chord produces a local lift proportional to the local chord squared. Since $c(y) \sim \sqrt{1 - (y/b)^2}$, the lift distribution $L(y) \sim 1 - (y/b)^2$.

Summarizing, the spanwise lift distribution is parabolic, the induced downwash in the wake is constant, and the wing is optimally loaded.

The lift coefficient of this wing is

$$C_L = \frac{\alpha}{\varepsilon} \frac{8}{3\pi} \frac{b^2}{b^2+1} \tag{5.12}$$

This is plotted in Figure 13.

The semi-circular wing, b = 1, has half the lift of the infinite wing. The theory is not valid for aspect ratios of the order of the clearance but this is not a practical limitation. The aerodynamic center for this wing is at the 41% chord, measured from the root leading edge.

The results for $b/c \to \infty$ do not approach the two-dimensional results since the wing remains elliptic in this limit. Although the flow becomes locally two-dimensional, since the outboard chords are shorter in comparison to their height above the ground, the lift decreases in proportion to the square of the local chord in contrast to the infinite fluid case. For a two-dimensional wing to lowest order

$$C_{L_{2D}} = \frac{\alpha}{\varepsilon} \tag{5.13}$$

whereas for $b/c \to \infty$

$$C_L = \frac{\alpha}{\varepsilon} \frac{8}{3\pi} \tag{5.14}$$

The matching procedure applied to the two-dimensional problem can also be applied locally to the edges of the three-dimensional wing. The perturbation velocities of $\phi_1^c(x,y)$ are normal to the leading and side edges and the two-dimensional edge flow solution can be applied to lowest order since the radius of curvature is of $O(1)$, which is large in comparison to the width of the edge flow region, of $O(\varepsilon)$. The details will not be carried out here; the results will be stated with reference to the two-dimensional results. The outer flow potential ϕ_1^o can be constructed from a known distribution of sources and sinks located over the wing and wake. Matching the channel perturbation potential to this outer flow through local normal edge flows gives a boundary condition on $\frac{\partial \phi^c}{\partial x}$ at the trailing edge and ϕ^c at the leading edge.

At a point s on the leading edge the inner limit of the outer solution will be

$$\phi^{oi} \sim \frac{U(s)}{\pi} \log n - \frac{1}{\pi} [n \log n - A(s)] \tag{5.15}$$

where n is a local normal coordinate. U(s) is the local normal velocity, $\frac{\partial \phi_1}{\partial n}^c$. A(s) is the O(1) effect due to distant sources. Matching this expression through a local edge flow solution gives the boundary conditions for ϕ^c at the leading edge.

$$\phi^c(s) = - \frac{U(s)}{\pi} \log \frac{\pi}{\varepsilon} - \frac{U(s)}{\pi} + \frac{A(s)}{\pi} \tag{5.16}$$

Similarly, for a trailing edge in three-dimensional flow, the outer flow solution will behave locally as

$$\phi_T^{oi} = \frac{(1 - \frac{\alpha_i}{\alpha})}{\pi} [x_T \log x_T] + B(y) + C(y)x_T \tag{5.17}$$

The first term comes from the discontinuity in sink strength at the trailing edge where the downwash changes from α to α_i as indicated in Figure 11. B(y) and C(y) are O(1) effects from distant sources. Matching this through a local trailing edge solution gives a boundary condition for $\frac{\partial \phi^c}{\partial x}$ at the trailing edge to O(1).

$$\frac{\partial \phi^c}{\partial x}(0) = - \frac{[1 - \frac{\alpha_i}{\alpha}]}{\pi} \log \frac{\pi}{\varepsilon} + C(y) \tag{5.18}$$

Restating the governing equations for the individual terms in the expansion of (2.7) for ϕ^c, the potential beneath the wing, we have

$$\nabla^2 \phi_1^c = 1 \tag{2.19}$$

$$\nabla^2 \phi_2^c = 0, \qquad \nabla^2 \phi_3^c = 0 \tag{2.20}$$

The matching has provided the boundary conditions for these equations to be applied at the leading and trailing edges. At a leading edge

$$\phi_1^c = 0$$

$$\phi_2^c = - \frac{1}{\pi} \frac{\partial \phi_1}{\partial n}^c$$

$$\phi_3^c = - \frac{1}{\pi} [1 + \log \pi] \frac{\partial \phi_1}{\partial n}^c \frac{A(s)}{\pi}$$

At a trailing edge

$$\frac{\partial \phi_1}{\partial x}^c = 0$$

$$\frac{\partial \phi_2}{\partial x}^c = -\left[1 - \frac{\alpha_i}{\alpha}\right] \frac{1}{\pi} \tag{5.20}$$

$$\frac{\partial \phi_3}{\partial x} = -\left[1 - \frac{\alpha_i}{\alpha}\right] \log \pi + C(y)$$

With these equations, the lifting surface problem for a wing in close proximity to the ground becomes a direct although perhaps tedious problem.

It is of interest to carry the semi-circular wing to next order. This can be done relatively simply because $\frac{\partial \phi_1}{\partial n}^c$ is constant around the leading edge for this particular case. Stating the problem for $\phi_2^c(x,y)$, we have

$$\nabla^2 \phi_2^c(x,y) = 0$$

$$\phi_2^c = -\frac{1}{2\pi} \quad \text{at the leading edge,} \tag{5.21}$$

$$\frac{\partial \phi_2}{\partial x}^c = -\frac{1}{2\pi} \quad \text{at the trailing edge.}$$

The solution can be found using complex variable image techniques.

Using $z = y - ix$ for convenience

$$\phi_2^c + i\psi_2^c = \frac{1}{2\pi^2}\left\{ -(z-1)\log(z-1) + \left(\frac{1}{z} - 1\right)\log\left(\frac{1}{z} - 1\right) + (z+1)\log(z+1) - \left(\frac{1}{z} + 1\right)\log\left(\frac{1}{z} + 1\right) - 2\log z \right\} - \frac{1}{2\pi}$$

The value of $\phi_2^c(y)$ along the trailing edge gives the additional circulation $\Gamma_2(y)$,

$$\Gamma_2(y) = -\alpha \ln \frac{1}{\epsilon} \phi_2^c = -\alpha \ln \frac{1}{\epsilon}\left(\frac{1}{2\pi^2}\left(\frac{1-y^2}{y}\right)\log\frac{1-v}{1+y} - \frac{1}{2\pi}\right) \tag{5.23}$$

The additional contribution to the lift is

$$C_{L_2} = \alpha \ln\left(\frac{1}{\epsilon}\right) \frac{4}{\pi}\left(\frac{1}{4} + \frac{1}{\pi} - \frac{1}{\pi^2}\right) \tag{5.24}$$

For a circular wing to $O(\alpha \ln \epsilon)$

$$C_L = \frac{\alpha}{\epsilon}\frac{4}{3\pi} + \alpha \ln\left(\frac{1}{\epsilon}\right)\left(\frac{4}{\pi}\right)\left(\frac{1}{4} + \frac{1}{\pi} - \frac{1}{\pi^2}\right) \tag{5.25}$$

The next term would be $O(1)$ and would involve contributions for both the upper and lower surfaces.

6. Comparison with Numerical Lifting Surface Theory

Numerical calculations for two elliptical wings with straight trailing edges in an infinite free stream and in ground effect were performed using the method discussed by Ashley, Widnall and Landahl (1965). Two wings were chosen having semispan to chord ratios of 1 and 0.5. The numerical method was developed for wings in an infinite fluid with moderate aerodynamic influence from nearby surfaces. It was felt that for this technique convergence could not be assured much below $\varepsilon = 0.05$. Of course, this region of strong influence is just where the analytic solution is expected to be valuable. The numerical results for lift coefficient are summarized in Figure 14.

For the wing in ground effect, $C_L\varepsilon/\alpha$ is plotted versus ε to focus on the behavior for small clearances. The first order linear theory predicts $C_L\varepsilon/\alpha$ to be a function only of aspect ratio. The limits for $b/c = 0.5$ and 1.0 are indicated at $\varepsilon = 0$. For large clearances C_L approaches the free stream limit C_{L_∞} so $C_L\varepsilon/\alpha$ increases linearly with ε. This asymptote, $C_{L_\infty}\varepsilon/\alpha$ is indicated in Figure 14. The results of the numerical lifting surface calculations for the two finite wings in ground effect are shown for $\varepsilon = 0.05$, 0.1, 0.3, and 0.5.

The numerical results indicate a reasonable approach to the $\varepsilon = 0$ limit. For finite values of ε, however, one is tempted to proceed to higher order in ε, the next terms in the expansion for $C_L\varepsilon/\alpha$ being $\sim O(\varepsilon \ln \varepsilon)$, and $O(\varepsilon)$. This proved to be quite easy for the semi-circular wing and the two-dimensional wing because the perturbation mass flow normal to the edges is constant.

The two-term expansion for the semi-circular wing as given by (5.25) is shown in Figure 14 and shows reasonable consistency with the numerical results, although one more term in the expansion would be required for the same quality of comparison as shown for the two-dimensional results.

A comparison of the lift distribution on a semicircular wing in ground effect as predicted by the simple first order theory and as obtained using numerical lifting surface techniques is shown in Figure 15 for a height to root chord ratio $\varepsilon = 0.05$.

The first order theory gives the simple linear lift distribution. The lifting surface result contains the proper leading and trailing edge behavior which would appear in the analytic solution for higher orders in ε as in the two-dimensional case. The agreement is quite good in those regions away from the edge.

7. Summary and Conclusions

Using the method of matched asymptotic expansions, the linearized lifting surface problem for a wing very close to the ground has been formulated. Unlike the lifting surface problem in an infinite fluid, the lifting problem close to the ground is a direct problem involving a source/sink rather than a vortex distribution. Flow in the confined region beneath the wing and wake is a two-dimensional channel flow with known boundaries and known mass addition, coming from the flow tangency boundary condition on the lower surfaces. The thickness and lifting problems do not decouple for a wing in strong ground effect, in fact, to lowest order the lift coefficient is only a function of the shape of the wing lower surface and planform.

The two dimensional linearized flow problem for a lifting flat plate close to the ground is particularly amenable to solution by this method. Analytic solutions may be obtained up to fourth order (i.e. $\varepsilon \ln \varepsilon$) without undue difficulty. Higher order terms are available, although their usefulness is questionable. The third order result for the pressure distribution on the upper and lower surfaces are remarkably accurate, showing good agreement with numerical calculations for clearances as large as $\varepsilon = 0.5$. The singularity at the leading edge shown by the flat plate solution could be removed by a method similar to Lighthill's technique for correcting flows around blunt leading edges.

A remarkably simple analytic solution is obtained in the case of an optimally loaded flat elliptical wing with a straight trailing edge. The lift distribution for minimum induced drag is a distribution which is linear along the chord, dropping to zero at the trailing edge to satisfy, to lowest order, the Kutta condition. An analytic expression (5.12) gives the lift coefficient of such a wing to $O(1/\varepsilon)$; this equation

is valid for all aspect ratios greater than ε.

For the semi-circular flat wing the flow perturbations can be found analytically to $O(\ln \varepsilon)$ giving a two term expansion for C_L. The analytical results are compared with numerical results from lifting surface theory for a finite wing in ground effect. For good accuracy up to $\varepsilon = 0.1$, the solution should be carried to $O(\alpha)$. In the expected range of operation of high speed ground transportation vehicles, say $\varepsilon = 0.01$, the simple first order solution should give accurate results.

The method of matched asymptotic expansions gives a very powerful approach to attack the wide variety of problems associated with lifting systems operating in close proximity to solid boundaries. The non-linear lifting problems in which the changes in the clearance due to angle of attack are of order of the clearance can be treated using this technique and some of the effects of viscosity in the inner channel flow region can also be incorporated.

REFERENCES

Ashley, H. and Landahl, M., (1965), Aerodynamics of Wings and Bodies, Addison Wesley, Reading, Massachusetts.

Ashley, H., Widnall, S. and Landahl, M., (1965), "New Direction in Lifting Surface Theory", AIAA Journal, vol. 3, no. 1, pp. 3-16.

Barrows, T. M., and Widnall, S. E. (1969), "Optimum Lift-Drag Ratio for a Ram Wing Tube Vehicle", submitted for publication AIAA Journal.

Van Dyke, M., (1964), Perturbation Methods in Fluid Mechanics, Academic Press Inc., New York.

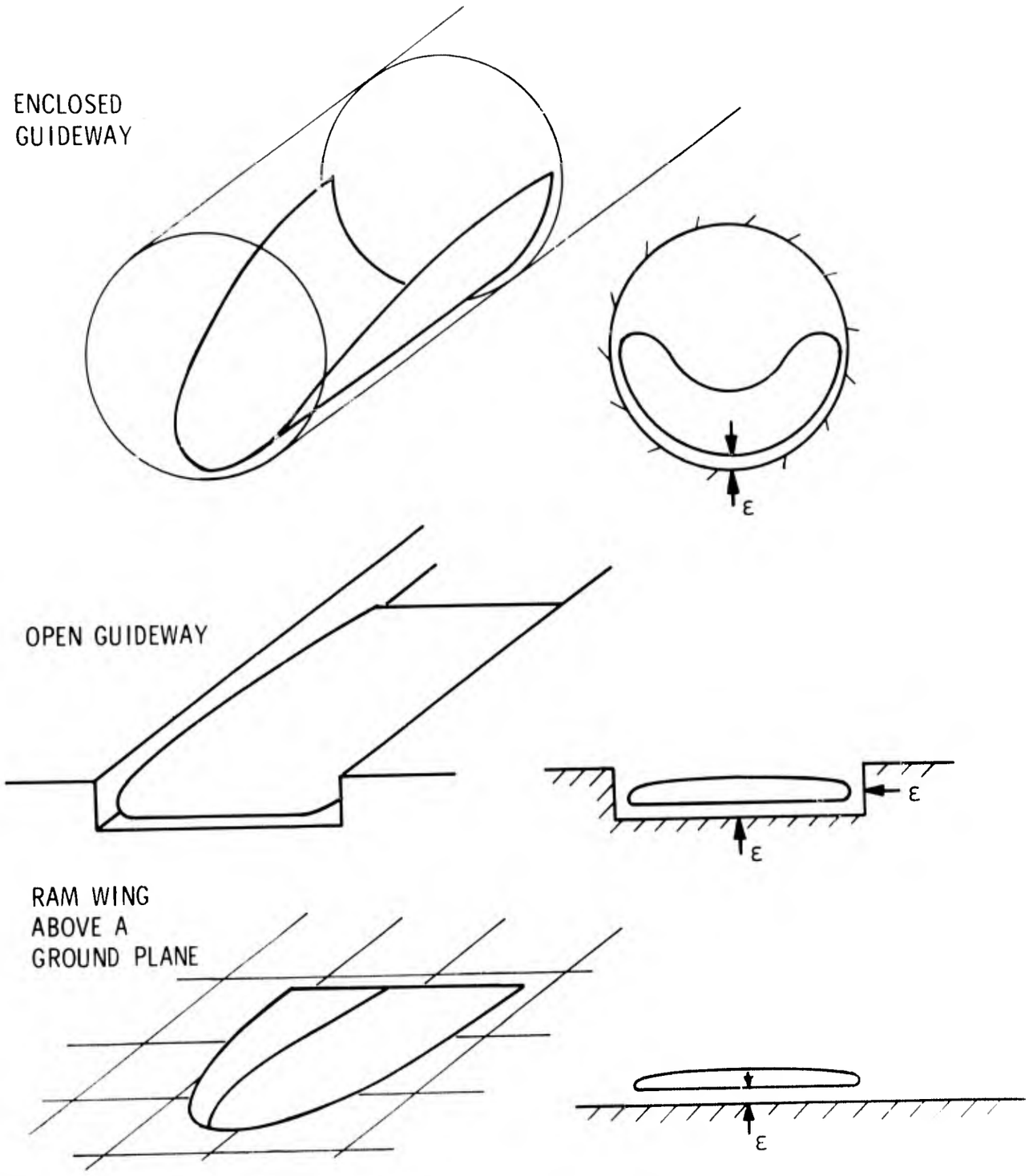

Fig. 1 HIGH SPEED GROUND TRANSPORTATION VEHICLES
IN CLOSE PROXIMITY TO SOLID BOUNDARIES

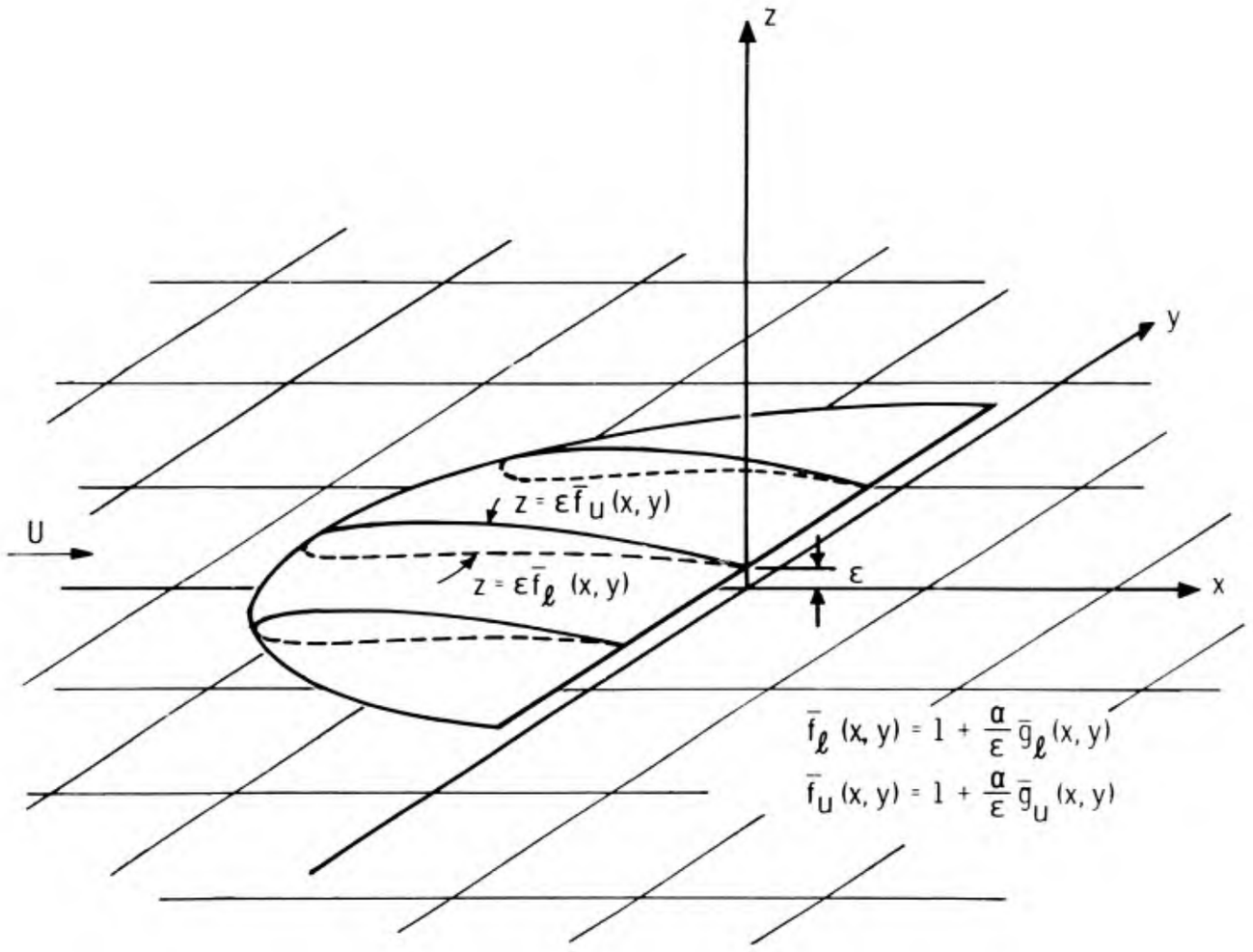

Fig. 2 LIFTING SURFACE IN CLOSE PROXIMITY TO THE GROUND

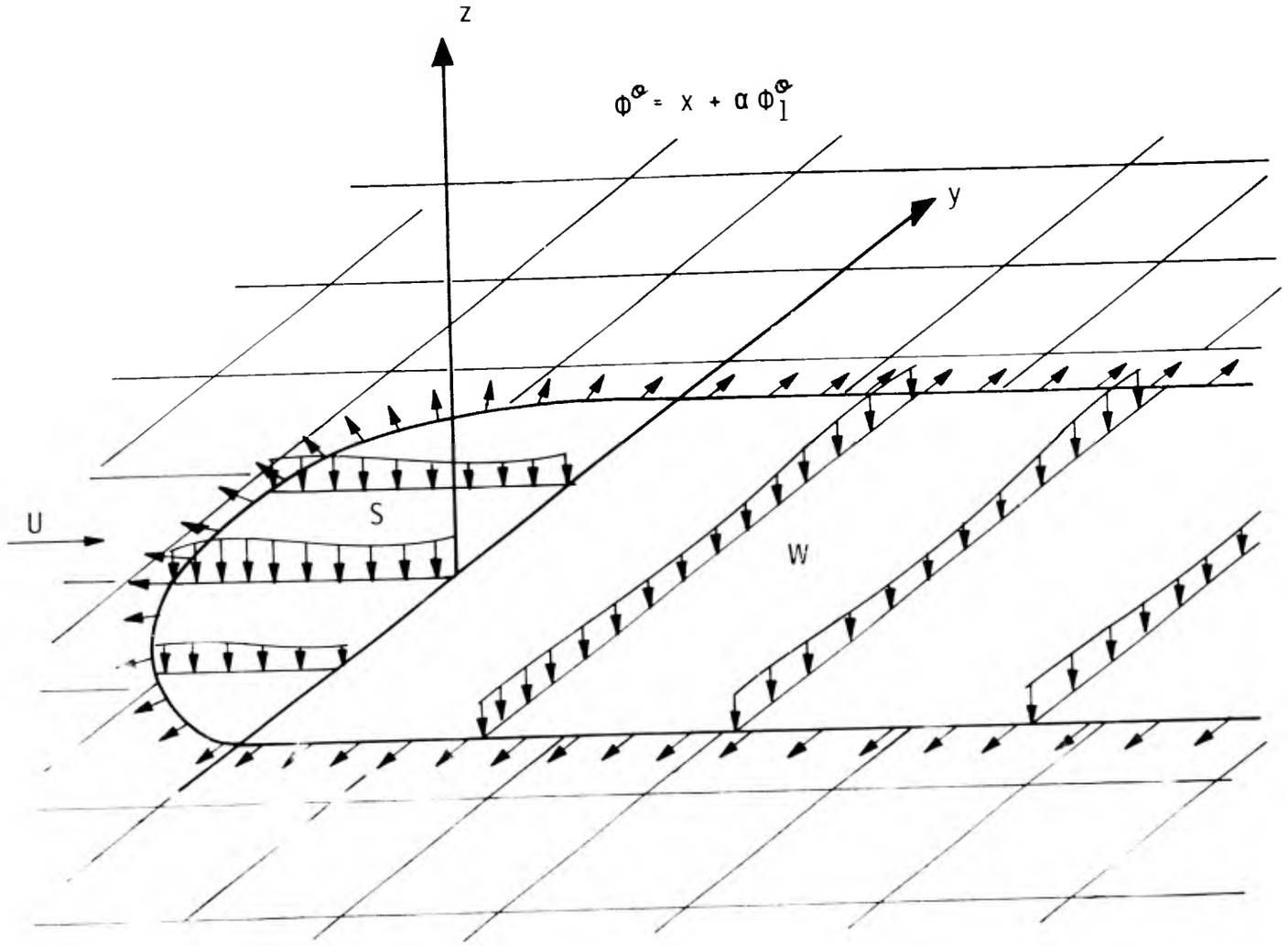

Fig. 3 SKETCH OF THE OUTER FLOW-
THE FLOW ABOVE THE WING IN THE LIMIT $\varepsilon \to 0$

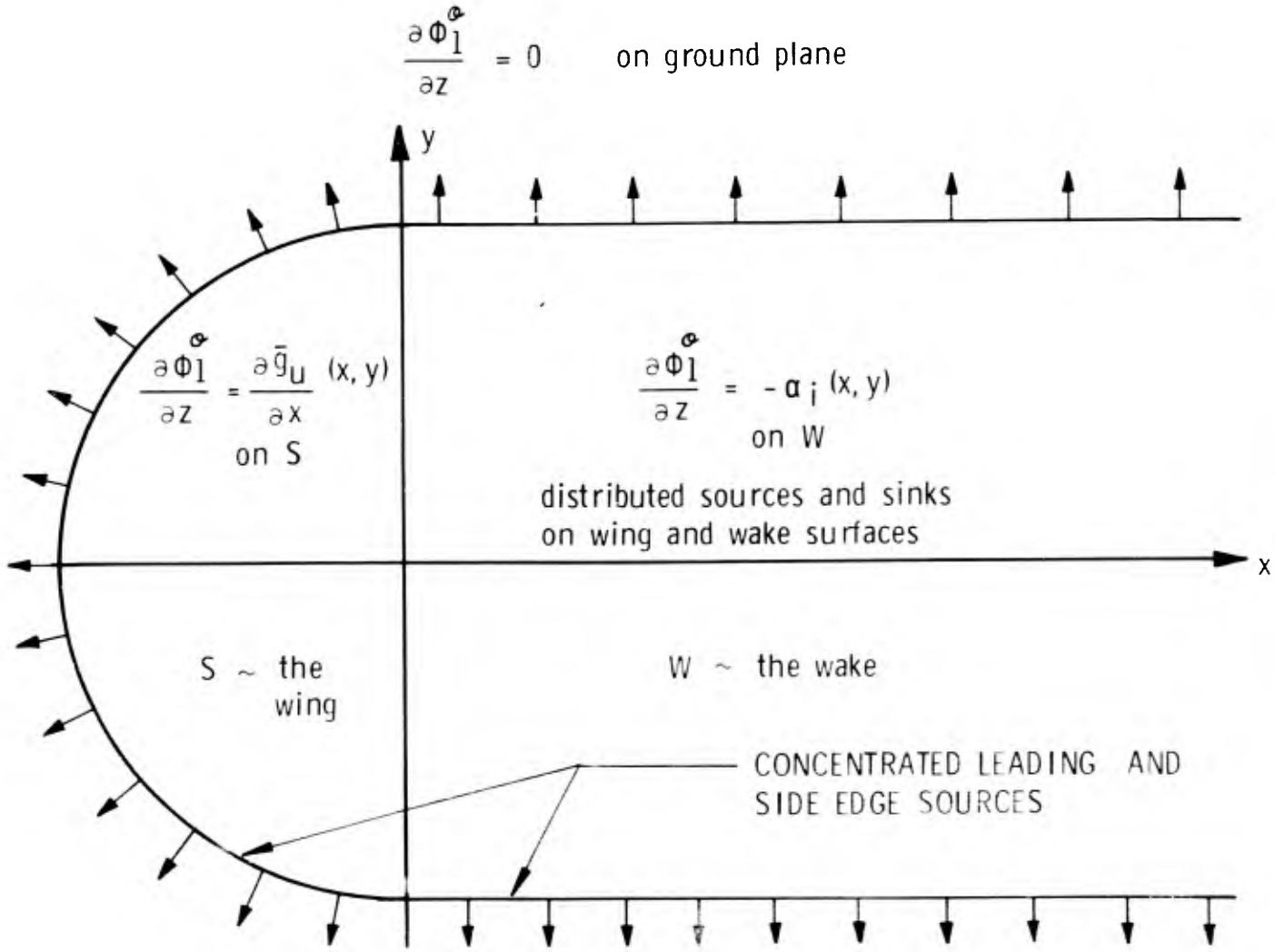

Fig. 4 BOUNDARY CONDITIONS TO BE SATISFIED AT z = 0 IN THE OUTER FLOW

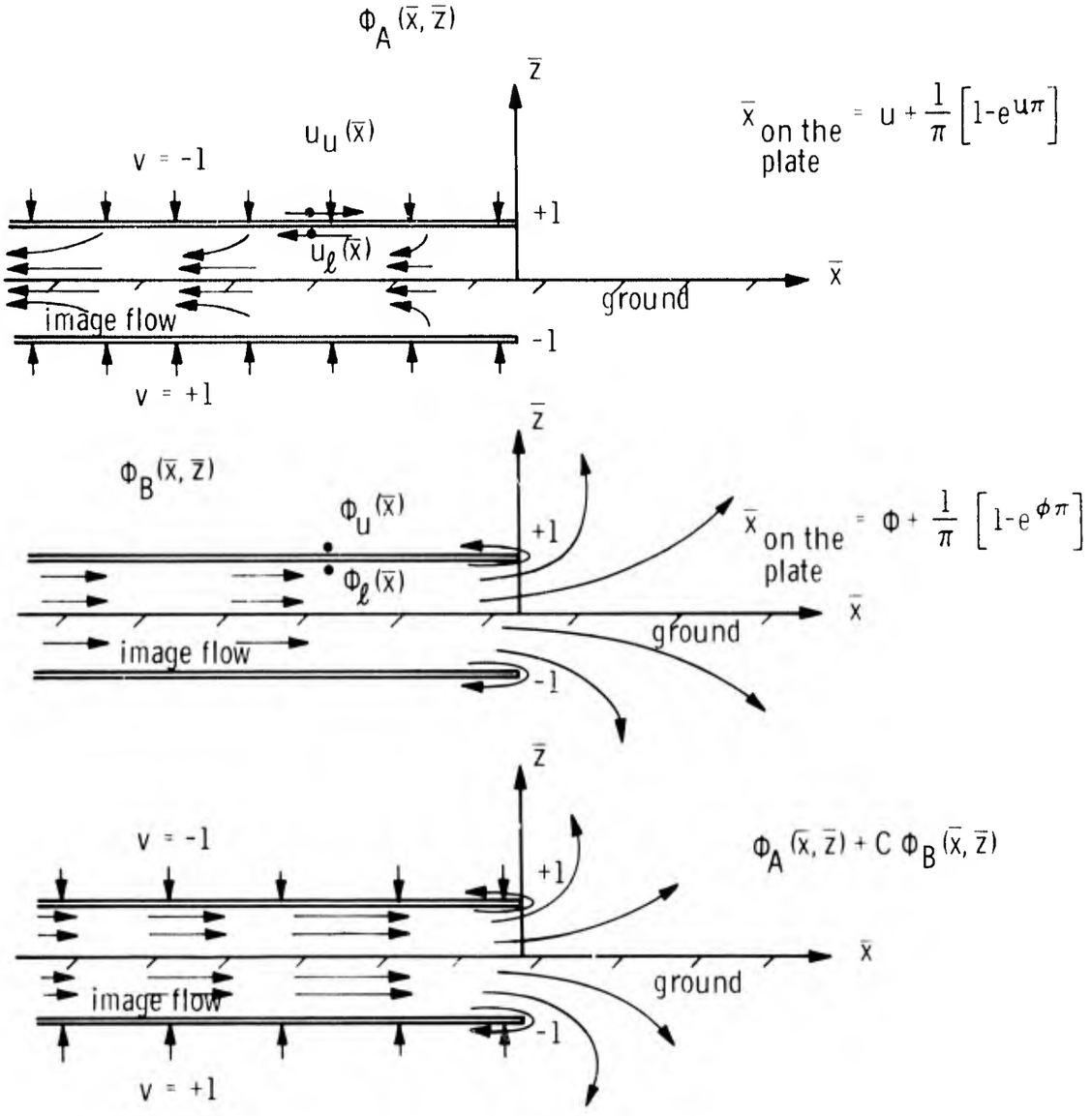

Fig. 5 TWO-DIMENSIONAL INCOMPRESSIBLE EDGE FLOW PROBLEMS VALID NEAR THE EDGE OF A FLAT WING IN GROUND EFFECT

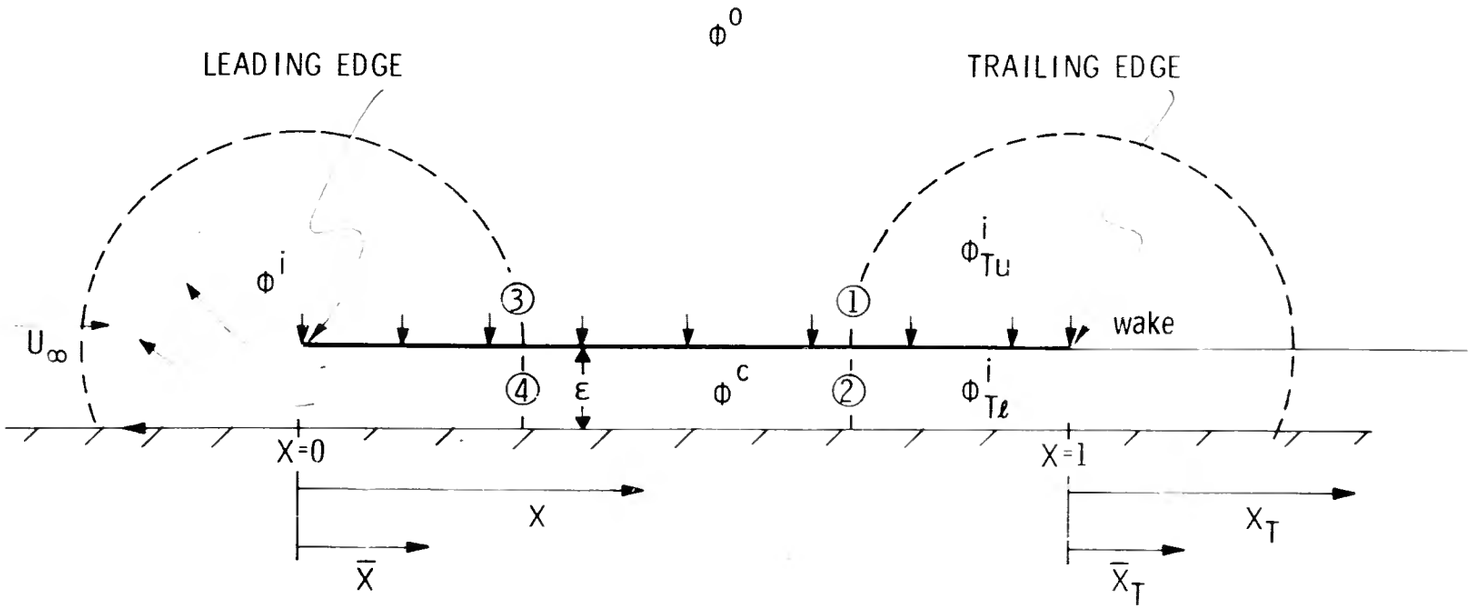

Fig. 6 ORDER OF MATCHING FOR THE TWO-DIMENSIONAL WING IN GROUND EFFECT

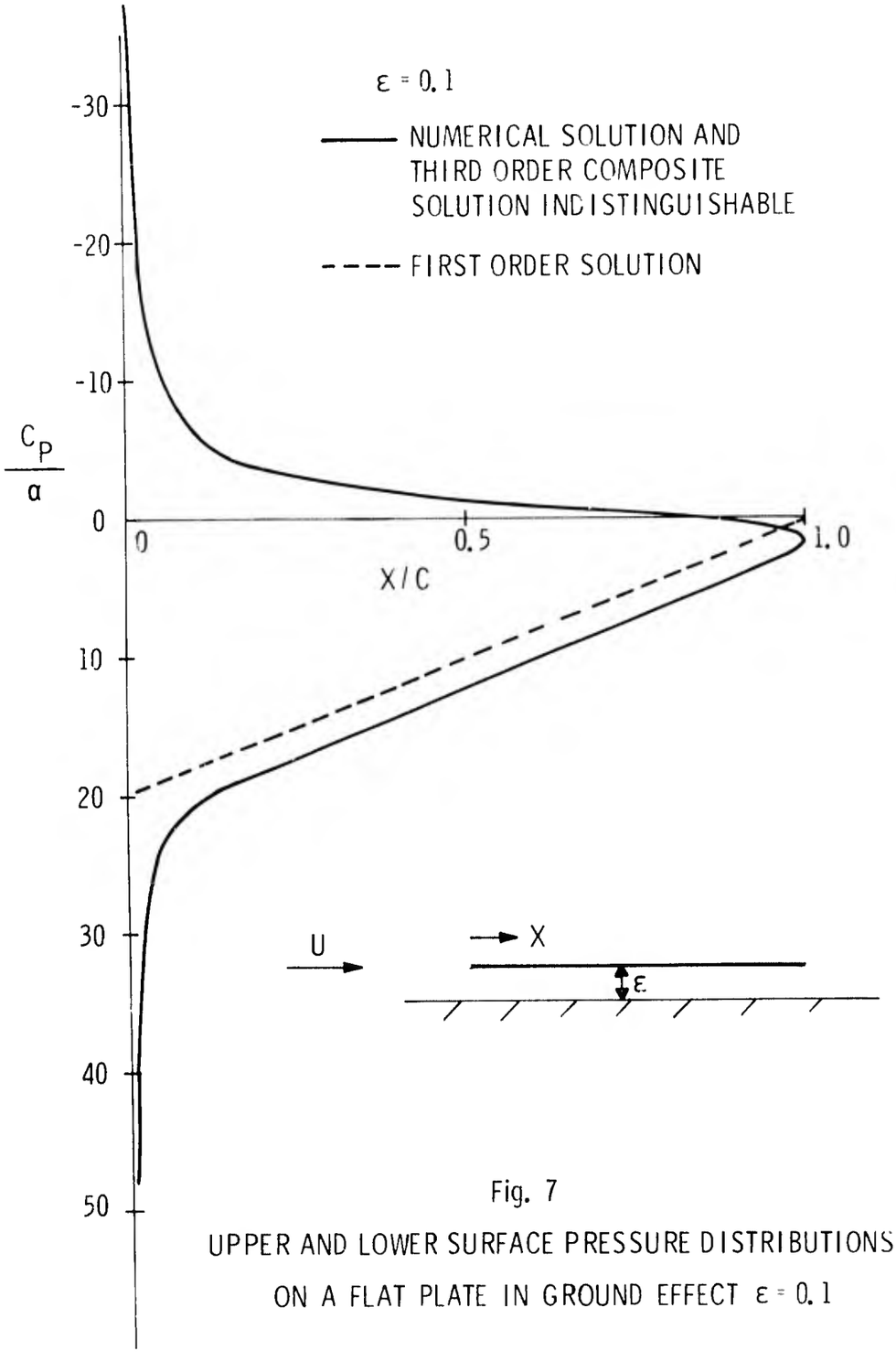

Fig. 7

UPPER AND LOWER SURFACE PRESSURE DISTRIBUTIONS ON A FLAT PLATE IN GROUND EFFECT $\varepsilon = 0.1$

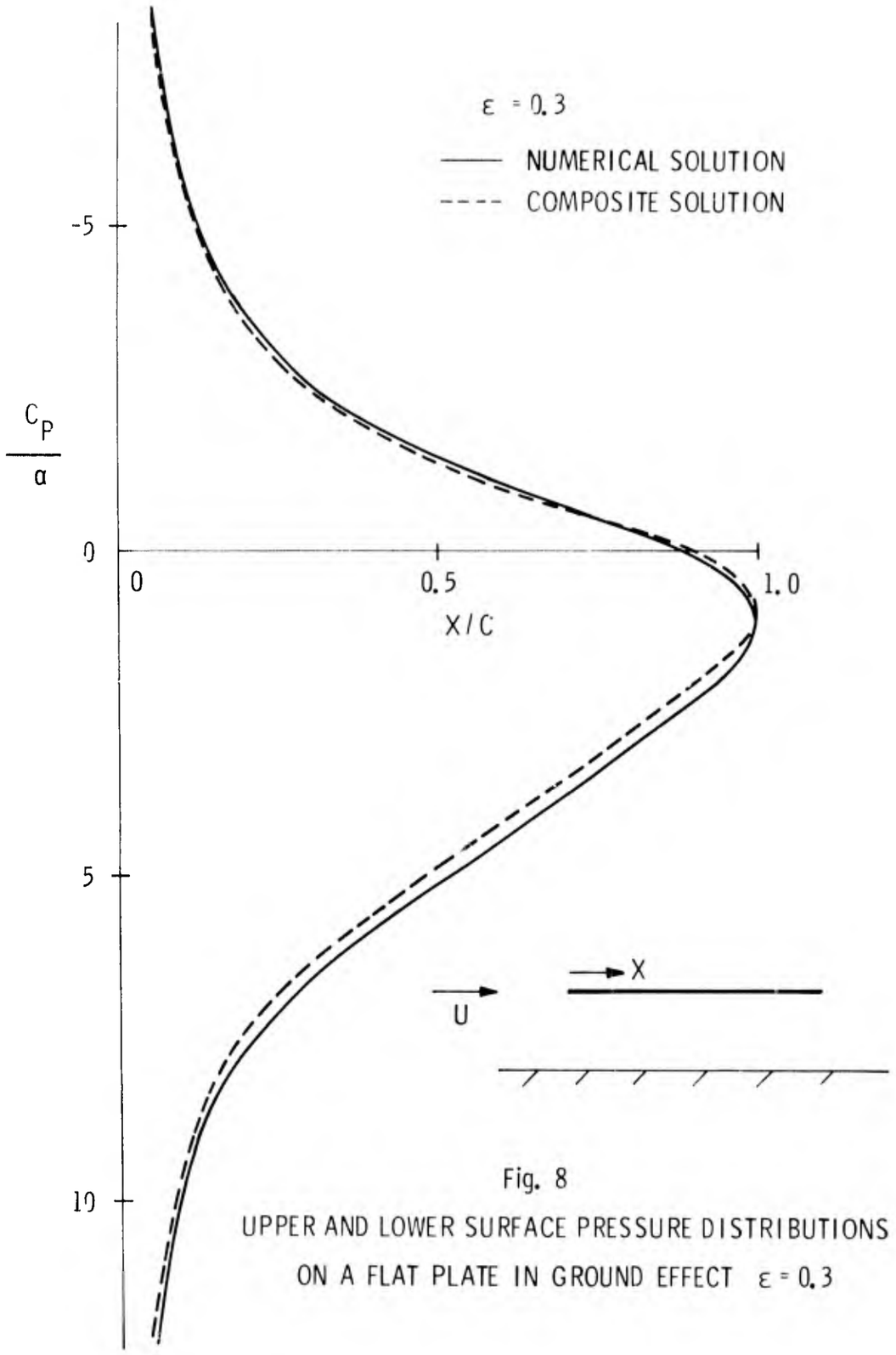

Fig. 8

UPPER AND LOWER SURFACE PRESSURE DISTRIBUTIONS ON A FLAT PLATE IN GROUND EFFECT $\varepsilon = 0.3$

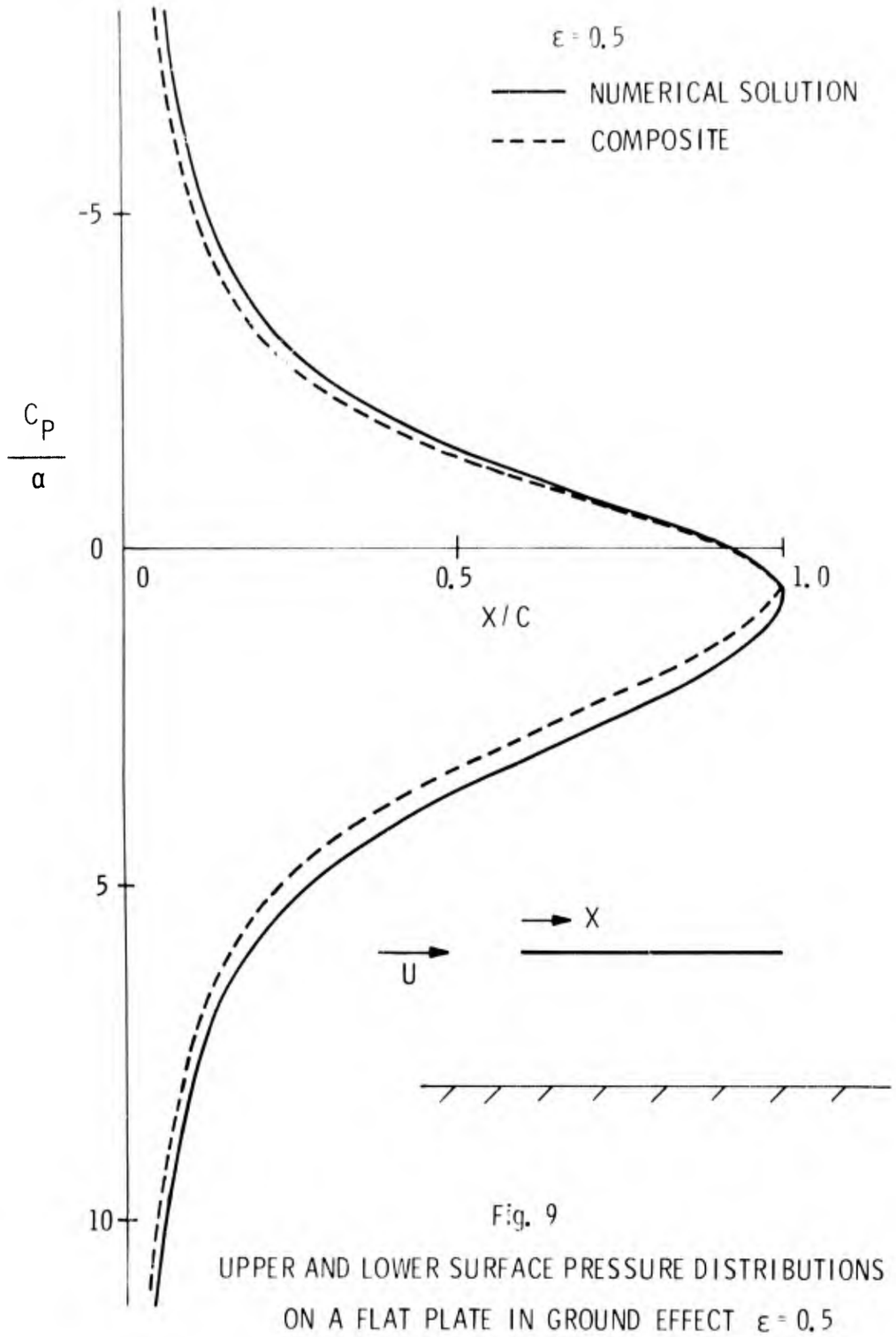

Fig. 9

UPPER AND LOWER SURFACE PRESSURE DISTRIBUTIONS ON A FLAT PLATE IN GROUND EFFECT $\varepsilon = 0.5$

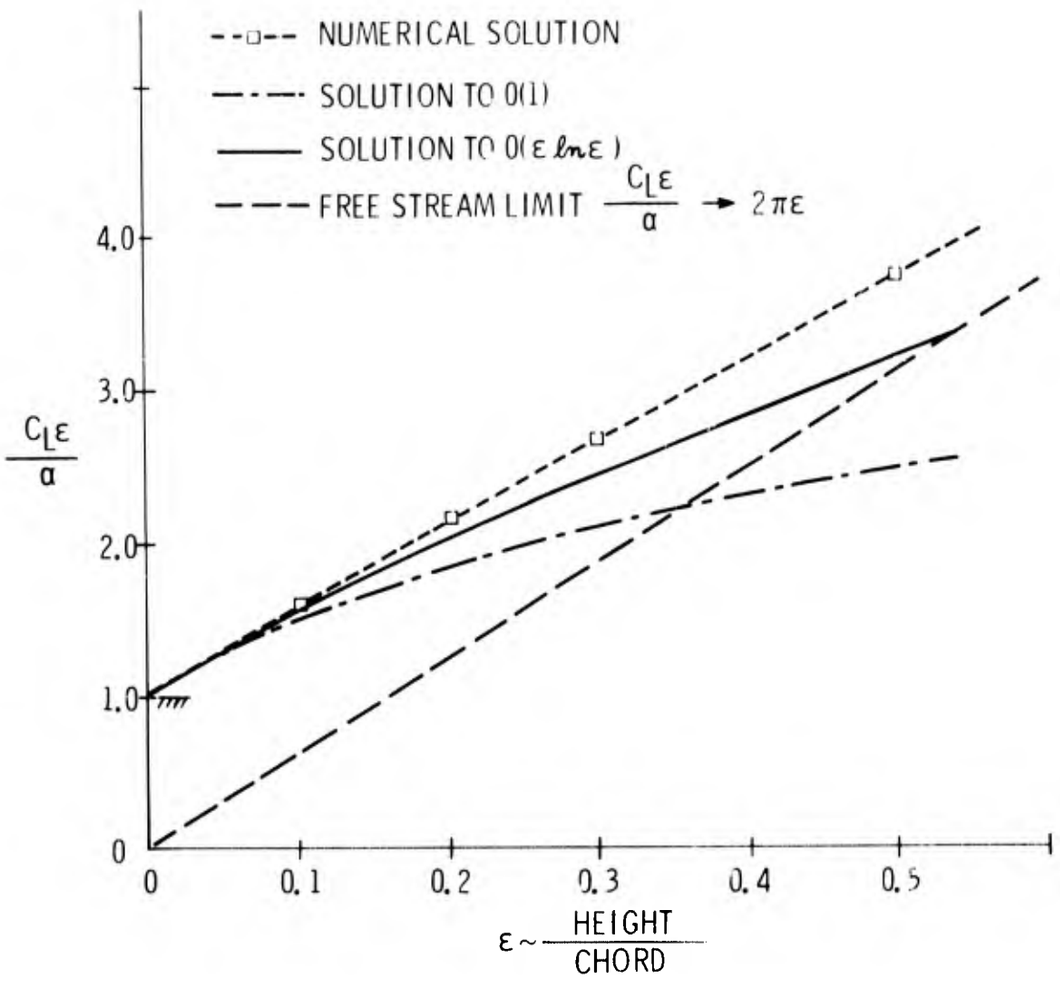

Fig. 10 LIFT COEFFICIENT FOR A TWO-DIMENSIONAL FLAT PLATE AIRFOIL IN GROUND EFFECT

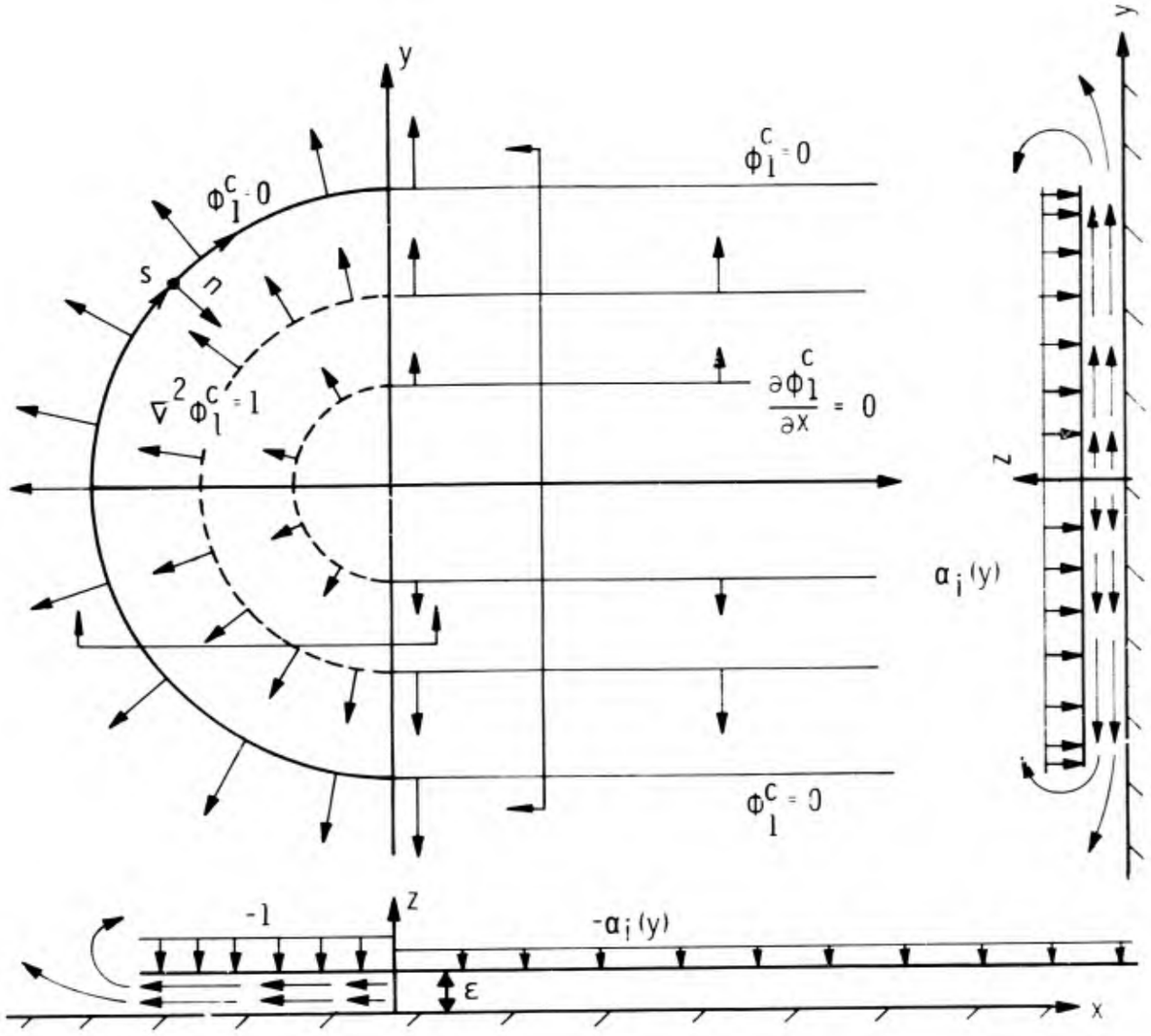

Fig. 11 FLOW PERTURBATIONS BENEATH A FLAT ELLIPTICAL WING WITH A STRAIGHT TRAILING EDGE DESCRIBED BY $\Phi_1^c(x, y)$

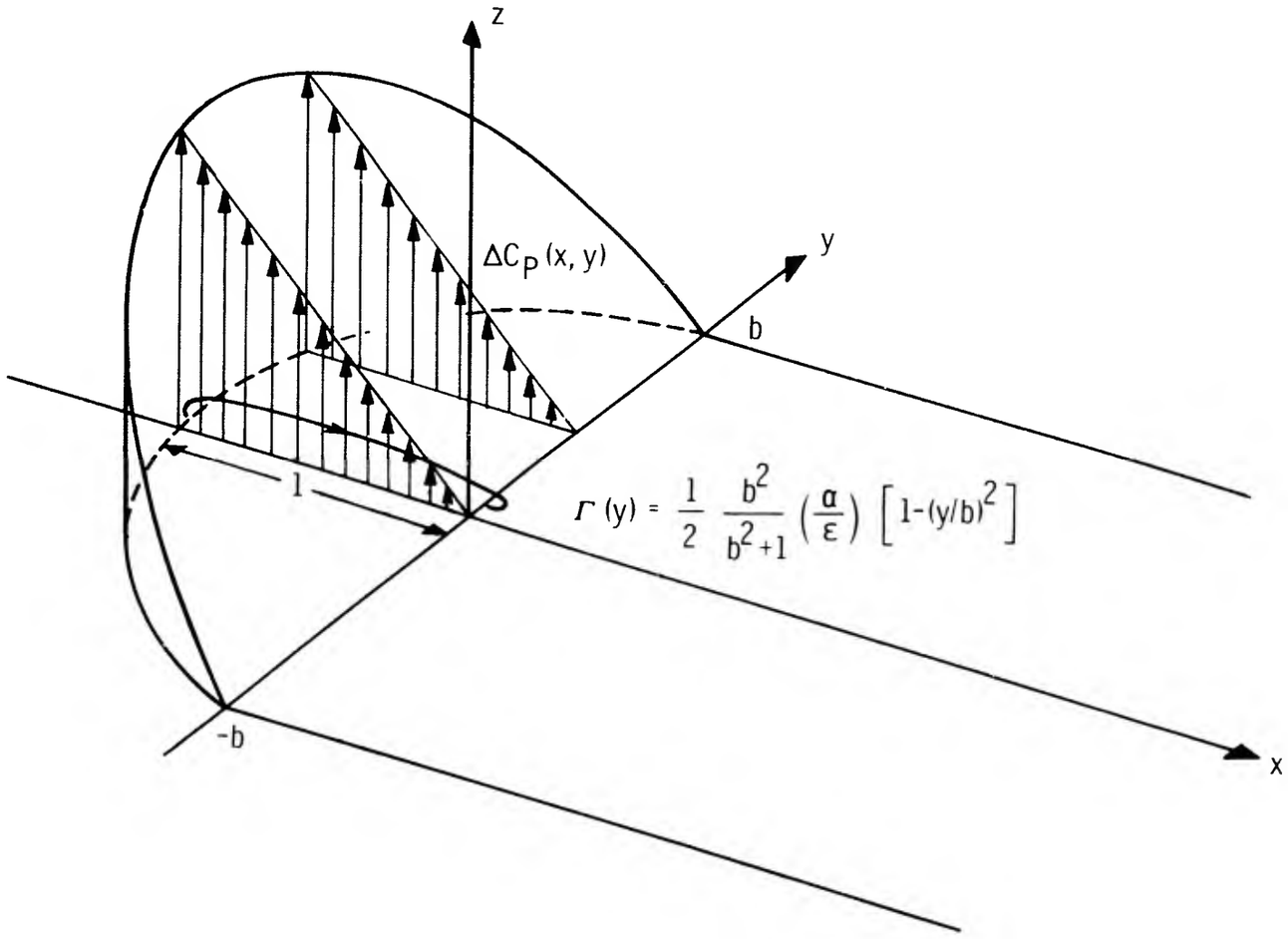

Fig. 12 LIFT DISTRIBUTION TO LOWEST ORDER ON AN OPTIMALLY LOADED WING VERY CLOSE TO THE GROUND

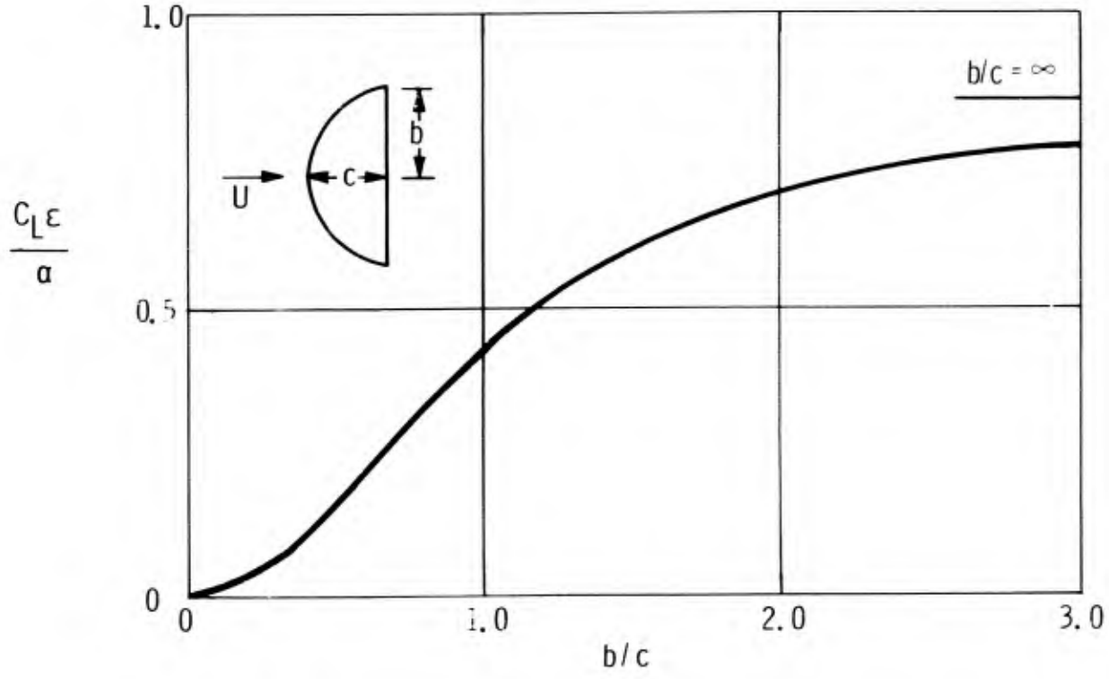

Fig. 13 THE LIFT COEFFICIENT FOR AN ELLIPTICAL FLAT WING IN CLOSE GROUND PROXIMITY. α- ANGLE OF ATTACK, ε- CLEARANCE, $\alpha \ll \varepsilon$

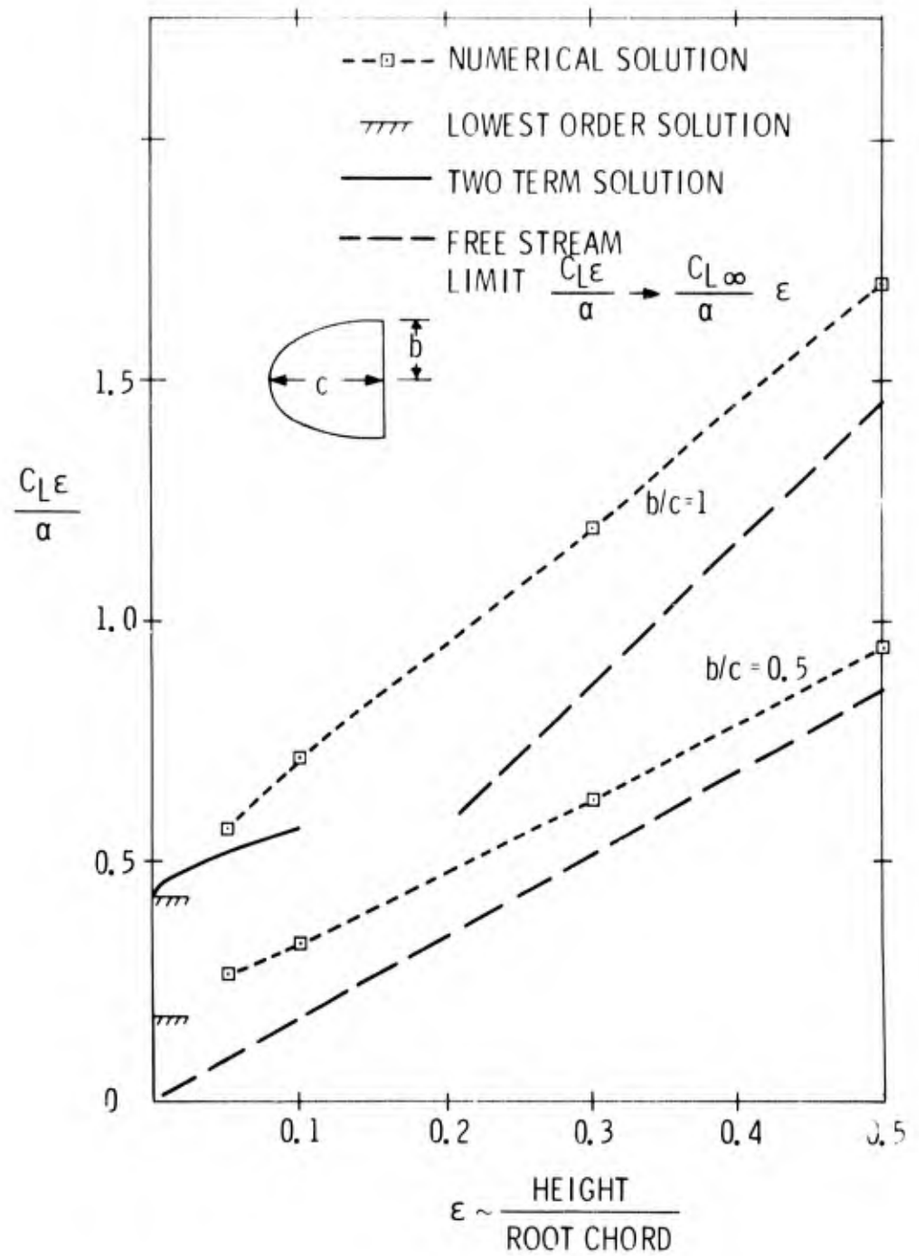

Fig. 14 COMPARISON OF NUMERICAL LIFTING SURFACE THEORY WITH THE ANALYTIC SOLUTION FOR A FLAT ELLIPTICAL WING IN GROUND EFFECT WITH CLEARANCE ε

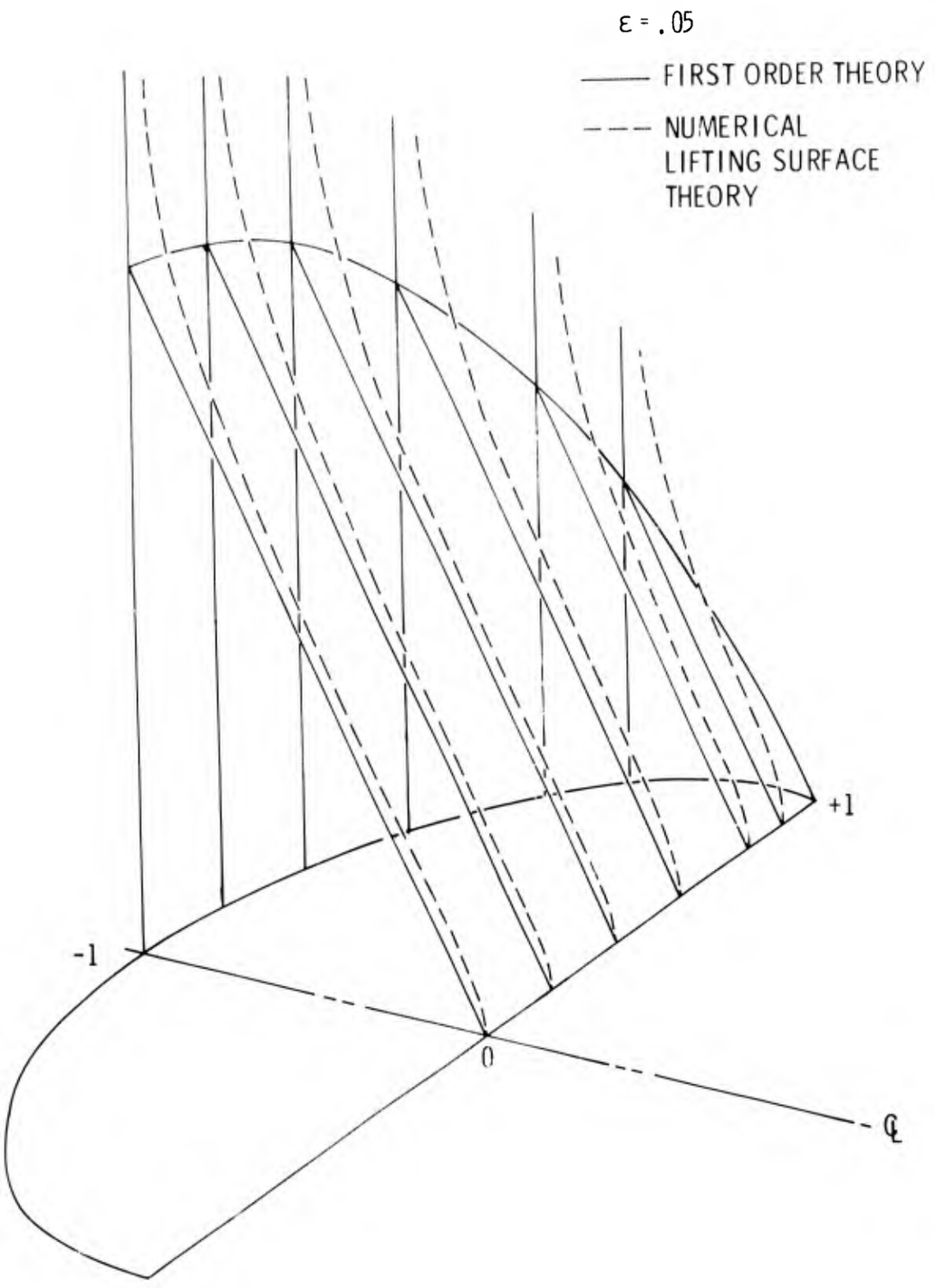

Fig. 15 COMPARISON OF ANALYTIC AND NUMERICAL RESULTS FOR LIFT DISTRIBUTION ON A SEMICIRCULAR WING IN GROUND EFFECT